A Novel Pan-tilt Motion Generator

TR-CIM-10-01 January 2010

Danial Alizadeh[†], Jorge Angeles[†] and Scott Nokleby[‡]

[†]Department of Mechanical Engineering and Centre for Intelligent Machines,
McGill University

[‡]Faculty of Engineering and Applied Science,
University of Ontario Institute of Technology

Abstract

A recurrent design task in robotics and mechatronics applications involves the driving of a link through pan and tilt motions independently. Design solutions encountered in serial robots usually feature two actuators in series, sometimes the axis of the motor shaft aligned with the driven axis, sometimes via a mechanism. However, in the design of parallel robots, where all motors are preferably located at the base, the serial array is not an option, which calls for creative solutions. Included in this report is a set of variants obtained from brainstorming sessions, which are then ordered in ascending complexity. To do this, a theoretical framework based on the concept of complexity is applied to rank the variants from simplest to most complex. The simplest solution, which is a five-bar mechanism, is then chosen to go into the embodiment phase. It is noteworthy that the mobility analysis of the five-bar mechanism is elusive to the popular Chebyshev-Grübler-Kutzbach formula; the mechanism turns out to be of the *exceptional* type according to Hervé's classification based on group theory.

Contents

1 Introduction

A pan-tilt motion generator (PTMG) is a mechanism that produces two independent rotations, one about a vertical, one about a horizontal axis. The former is referred to as pan motion, the latter as tilt motion. PTMGs have been used in various applications, namely, industrial robots; orienting objects, such as cameras, telescopes and antennas (Carricato and Parenti-Castelli, 2004; Gogu, 2005; Vertechy and Parenti-Castelli, 2006; Hervé, 2006); and humanoid robots (Iwashita and Asada, 2005). In industrial robots, the pan and the tilt motions are produced by means of the actuation of two cascaded revolute joints forming a serial PTMG. However, carrying one actuator on top of the other entails some drawbacks, namely, increasing size, reducing accuracy and limiting speed. These drawbacks can be eliminated by using a parallel PTMG because its actuators are mounted on the base platform, thus reducing the weight of the moving links, while increasing speed and accuracy.

Researchers have extensively studied algorithms to choose the most suitable design among several alternatives at the conceptual design stage, where no parametric model is available (Saaty, 1980; Pugh, 1991; Hyman, 2003; Pahl et al., 2007). A framework recently proposed for ranking different alternatives in robot design sorts the alternatives in ascending order of complexity, the winning candidate being the least complex mechanism. Khan (2007) defined *design complexity* as a measure of the amount of information content required to obtain a desired functional performance. In this light, the design complexity of mechanical systems is considered to be proportional to the *diversity* of their components, namely, links, joints and actuators. Thus, computing the complexity of mechanical systems calls for quantifying component diversity. To this end, Khan et al. (2006) defined the *loss of regularity* (LOR) of lower and higher kinematic pairs as the ratio between the 2-norm of the curvature variation of the wrapping or, correspondingly, mating surfaces and the 2-norm of the curvature itself, both norms understood in a space of functions. Normalizing the LOR of each kinematic pair, the associated complexity, which varies between zero and unity, is obtained. The other instances of diversity, such as the link and the actuator diversity, can be quantified likewise. Finally, the overall complexity of the mechanism under study can be computed as a convex combination of the different partial complexity measures.

In this report, a number of parallel PTMGs resulting from brainstorming sessions are described. The proposed designs are compared based on the concept of design complexity so as to select the simplest mechanism, which turns out to be a five-bar linkage. This mechanism is overconstrained; therefore, the Chebyshev-Grübler-Kutzbach formula fails to compute its degree-of-freedom (DOF). The mechanism, indeed, belongs to the *exceptional* type, according to Hervé's classification (Hervé, 1978; Angeles, 2004), its DOF being one.

This report is organized as follows: in Section 2, a number of parallel PTMGs are introduced. Next, the concept of complexity is briefly recalled. The mechanisms are then compared in terms of their complexity and the winning mechanism is determined. The report closes with conclusions.

2 Mechanism Synthesis

Parallel PTMGs have certain advantages, namely, compactness, higher accuracy and higher stiffness over their serial counterparts. These benefits are achieved via mounting all actuators on the same base. In this section, we enumerate parallel PTMGs with two actuators, one for the pan, one for the tilt, both mounted on the same base.

It is desired to have two identical actuators. All proposed designs, except for the last one, satisfy this requirement. Among the five designs with identical motors, the first four produce the pan and the tilt motions by resorting to a planetary gear train, which consists of a sun, two planets, a ring gear and a planet carrier, as illustrated in Fig. 1. Actuating the sun and the ring gears, the pan motion is directly obtained from the rotation of the planet carrier, while an intermediate mechanism is required to transmit the rotation of the planet about its own vertical axis to the tilt shaft of horizontal axis.

Let us denote the angular velocities of the sun, the ring and the planet gears with ω_S, ω_R and ω_P, and their numbers of teeth with N_S, N_R and N_P, respectively. The pan rate, ω_1, which equals the angular

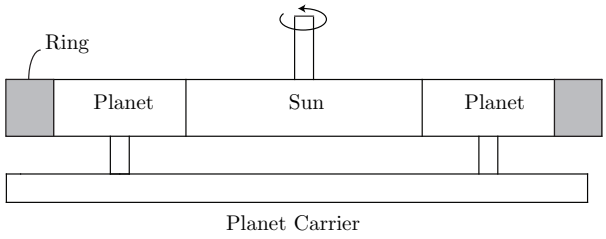

Figure 1: Planetary gear train

velocity of the planet carrier and the angular velocity of the planets, ω_P, are found as

$$\omega_1 = \frac{1}{m+1}\omega_R + \frac{m}{m+1}\omega_S \tag{1a}$$

$$\omega_P = \frac{1}{1-m}\omega_R - \frac{m}{1-m}\omega_S \tag{1b}$$

where $m = N_S/N_R$ is the gear ratio between the sun and the ring gears.

Next, various mechanisms for producing the tilt motion from the rotation of the planet about its vertical axis are described:

1. **Bevel-gear train**

   Bevel gears can transmit rotation between two intersecting axes. Thus, a pair of bevel gears can be simply implemented in order to transmit the rotation of the planet to the tilt shaft. In this case, the tilt angular velocity ω_2 can be computed as

   $$\omega_2 = n\omega_P \Rightarrow \omega_2 = \frac{n}{1-m}\omega_R - \frac{nm}{1-m}\omega_S \tag{2}$$

   in which $n = N_{B1}/N_{B2}$ denotes the gear ratio between the two gears.

   Casting eqs. (1a) and (2) in vector form, the Jacobian between the input and the output rates is derived as:

   $$\boldsymbol{\omega}_o = \mathbf{J}\boldsymbol{\omega}_i, \tag{3a}$$

   where

   $$\boldsymbol{\omega}_o = \begin{bmatrix}\omega_1 \\ \omega_2\end{bmatrix}, \boldsymbol{\omega}_i = \begin{bmatrix}\omega_R \\ \omega_S\end{bmatrix}, \mathbf{J} = \begin{bmatrix}\frac{1}{m+1} & \frac{m}{m+1} \\ \frac{n}{1-m} & \frac{-nm}{1-m}\end{bmatrix} \tag{3b}$$

   This Jacobian is constant, which is desirable, to simplify the control algorithm.

2. **Homokinetic joints**

   A homokinetic joint, a.k.a. constant velocity (CV) joint, is a kinematic coupling between two intersecting shafts transmitting the angular velocity, torque and power with a 1:1 ratio (Bellomo and Montanari, 1978). Such joints can be used to produce the tilt motion from the rotation of the planet; two instances are considered here.

(a) **Double universal joint**

Universal joints can transmit the rotation between two intersecting shafts; however, the ratio between the output and the input angular velocities varies with the rotation of the input shaft as (Johnson and Willems, 1993):

$$\frac{\omega_{\text{out}}}{\omega_{\text{in}}} = \frac{\cos\beta}{1 - \sin^2\beta\sin^2\theta} \tag{4}$$

where ω_{out} and ω_{in} are the output and the input angular velocities, while β and θ denote the angle between the two shafts and the angle of rotation of the input shaft. From eq. (4), a singularity of the universal joint is identified, which occurs when the two axes are orthogonal, at $\beta = \pi/2$.

Although a single universal joint is not homokinetic, the constant 1:1 velocity ratio between two intersecting axes with angle β can be achieved via two universal joints in series, each making an angle of $\beta/2$ with the intermediate shaft (Johnson and Willems, 1993).

A pair of universal joints is capable of producing the tilt motion from the rotation of the planet, as illustrated in Fig. 2. The axis of the input shaft of the first universal joint makes an angle of 45° with the intermediate shaft, which in turn makes an angle of 45° with the output shaft. Since the double universal joint is homokinetic, the tilt rate equals the angular velocity of the planet, expressed in eq. (1b). Hence, the relation between the input and the output rates is

$$\boldsymbol{\omega}_o = \mathbf{J}\boldsymbol{\omega}_i, \tag{5a}$$

where

$$\boldsymbol{\omega}_o = \begin{bmatrix}\omega_1\\ \omega_2\end{bmatrix}, \boldsymbol{\omega}_i = \begin{bmatrix}\omega_R\\ \omega_S\end{bmatrix}, \mathbf{J} = \begin{bmatrix}\dfrac{1}{m+1} & \dfrac{m}{m+1}\\ \dfrac{1}{1-m} & \dfrac{-m}{1-m}\end{bmatrix} \tag{5b}$$

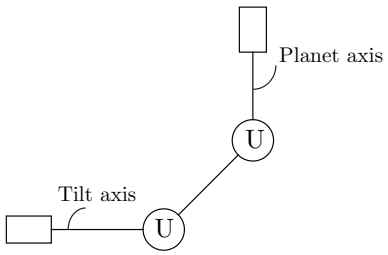

Figure 2: Double universal joint mechanism

(b) **Rzeppa joint**

The Rzeppa joint, whose parts are displayed in Fig. 3, is a homokinetic joint which can transmit motion between two intersecting shafts (Rzeppa, 1934). As shown in Fig. 3, the Rzeppa joint consists of an inner race, an outer race, a cage and six balls. The balls move inside six grooves located on the external and the internal peripheries of the inner and the outer races, respectively. The cage is mounted between the two races so as to keep the balls inside the grooves. The rotation of the input shaft, attached to the inner race, is transmitted to the output shaft, which is attached to the outer race, through the motion of the balls. The maximum angle allowed between the two shafts is about 50°; hence, two Rzeppa joints should be implemented in series so as to transmit motion uniformly between two orthogonal shafts. Therefore, the tilt motion can be achieved upon connecting the shaft of the planet to a double Rzeppa joint mechanism.

It is noteworthy that there are other types of homokinetic joints, such as the tripod and the Thomson joints, which can replace Rzeppa joints in the preceding design.

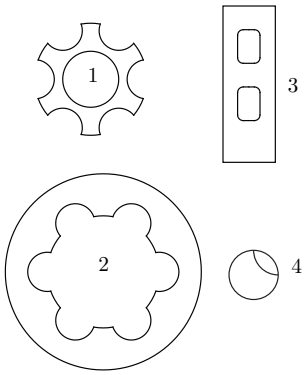

Figure 3: Rzeppa joint: 1) inner race; 2) outer race; 3) cage; 4) ball

3. **Five-bar linkage**

Shown in Fig. 4 is a novel PTMG, which uses a five-bar linkage to produce the tilt motion from the rotation of the planet. As shown in Fig. 5, the planet drives the ball-screw with an angular velocity ω_P, which in turn translates the slider 2; the latter rotates the tilt shaft at point D. The five-bar linkage is of the RHRRR type, where R and H denote revolute and helical pairs, respectively.

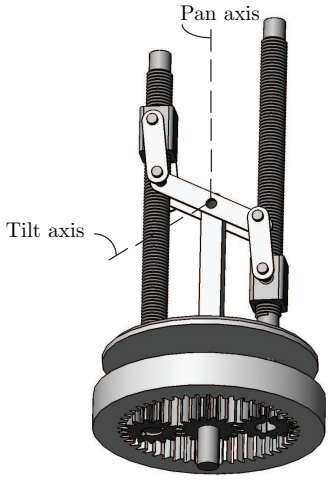

Figure 4: The CAD model of the five-bar linkage

Before proceeding to derive the input/output (I/O) velocity relations, we have to ensure that the five-bar linkage has a DOF = 1. However, the five-bar linkage is an overconstrained mechanism, and hence, the well-known Chebyshev-Grübler-Kutzbach formula fails to compute its DOF. In fact, according to Hérve's classification, this mechanism is of the *exceptional* type; its DOF should be computed by resorting to Hervé's methodology, based on group theory (Hervé, 1978; Angeles, 2004). Having numbered the links of the five-bar linkage in Fig. 5, two kinematic bonds between link 0 and link 2, denoted by $\mathcal{L}_J(0,2)$ for $J = I, II$, are found as:

$$\begin{aligned} \mathcal{L}_I(0,2) &= \mathcal{R}(\mathbf{e},A) \bullet \mathcal{H}(\mathbf{e},A) = \mathcal{C}(\mathbf{e},A) \\ \mathcal{L}_{II}(0,2) &= \mathcal{R}(\mathbf{n},D) \bullet \mathcal{R}(\mathbf{n},C) \bullet \mathcal{R}(\mathbf{n},B) = \mathcal{F}(\mathbf{n}) \end{aligned} \tag{6}$$

where $\mathcal{R}(\mathbf{e},X)$, $\mathcal{H}(\mathbf{e},X)$ and $\mathcal{C}(\mathbf{e},X)$ denote the revolute, the helical and the cylindrical subgroups with axes parallel to the unit vector $\mathbf{e}$ and passing through point X. Moreover, $\mathcal{F}(\mathbf{n})$ represents the planar subgroup with its normal parallel to the unit vector $\mathbf{n}$. Since the two unit vectors $\mathbf{n}$ and $\mathbf{e}$ are

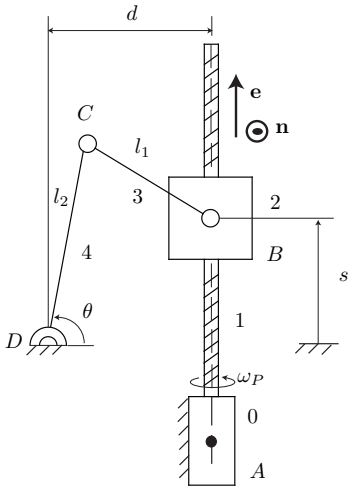

Figure 5: The schematic of the five-bar linkage

orthogonal, the intersection of the two kinematic bonds is

$$\mathcal{L}_I(0,2) \cap \mathcal{L}_{II}(0,2) = \mathcal{P}(\mathbf{e}) \tag{7}$$

where $\mathcal{P}(\mathbf{e})$ is the prismatic subgroup whose direction is parallel to the unit vector $\mathbf{e}$. The DOF of the five-bar linkage equals the dimension of the prismatic subgroup, which is unity.

The relation between the pan and the tilt rates and the angular velocities of the inputs is:

$$\boldsymbol{\omega}_o = \mathbf{J}\boldsymbol{\omega}_i, \tag{8a}$$

where

$$\boldsymbol{\omega}_o = \begin{bmatrix} \omega_1 \\ \omega_2 \end{bmatrix}, \boldsymbol{\omega}_i = \begin{bmatrix} \omega_R \\ \omega_S \end{bmatrix}, \mathbf{J} = \begin{bmatrix} \dfrac{1}{m+1} & \dfrac{m}{m+1} \\ \dfrac{k}{1-m} & \dfrac{-km}{1-m} \end{bmatrix}, \tag{8b}$$
$$k = \frac{\lambda \sin\theta - \sigma}{\delta \sin\theta - \sigma \cos\theta}\eta$$

where $\lambda = l_2/l_1$, $\sigma = s/l_1$, $\delta = d/l_1$ and $\eta = p/l_2$ are dimensionless parameters. Parameter p denotes the pitch of the screw, while θ, l_1, l_2, s and d are shown in Fig. 5. As the Jacobian obtained for this mechanism is variable, it should be inverted online to achieve the desired pan and tilt rates.

4. **Spherical linkage**

   Using a spherical linkage is another novel idea to produce the tilt out of the rotation of the planet about its vertical axis. The spherical linkage should be designed such that its output and input shafts are orthogonal, while the velocity ratio should be as close to 1:1 as possible, the slight variations being taken into account, again, by online Jacobian-inversion. It is desirable to have a tilt angle lying between $\alpha_{\min}$ and $\alpha_{\max}$ with respect to the vertical, which can be achieved with an output rocker.

   An example of a possible spherical linkage is displayed in Fig. 6. The velocity ratio between the output and the input angular velocities is approximately constant and equal to 2:1. This constant ratio is possible at the expense of the angle swept, $\alpha_{\max} - \alpha_{\min}$, which is of 180° in the displayed linkage. However, a controller may still be needed to regulate the output to achieve exactly a constant velocity ratio.

5. **Differential gear train**

   This PTMG, first proposed in (Morozov and Angeles, 2007), relies on an alternative planetary gear train to that described at the outset. As shown in Fig. 7, it consists of five components: (1) the fixed

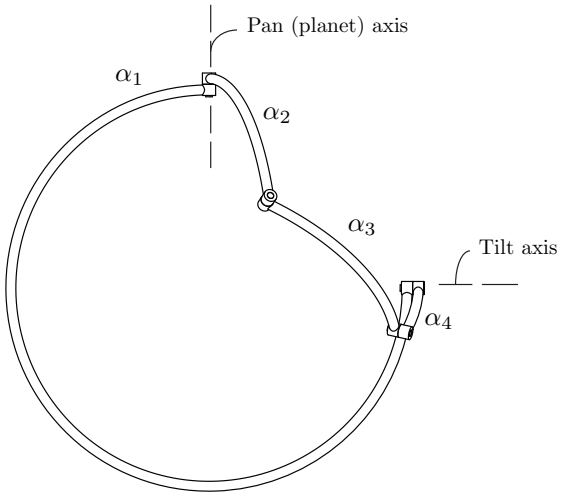

Figure 6: Spherical linkage

base; (2) the lower sun gear; (3) the upper sun gear; (4) the planets; and (5) the panning frame. The differential gear train is driven by two identical motors A and B. The lower sun gear is mounted on a hollow shaft and driven by motor A, while the shaft of the upper sun gear, actuated by motor B, passes through the hollow shaft; this layout allows the designer to put both motors on the base frame, at the bottom. The rotation of the moving frame about the vertical axis produces the pan motion, while the rotation of the planets about their axes gives the tilt motion. Denoting the angular velocities of motors A and B with ω_A and ω_B, the pan and the tilt rates, designated by ω_1 and ω_2, are found as

$$\omega_1 = \frac{n_A\omega_A + n_B\omega_B}{2}, \quad \omega_2 = \frac{m}{2}\left(n_B\omega_B - n_A\omega_A\right) \tag{9}$$

where $m = N_S/N_P$, n_A and n_B being the gear ratio between the sun and the planet and the reduction ratios between the angular velocities of motors A and B and their corresponding sun gears, respectively. The corresponding Jacobian is constant, as desired to ease the control. Moreover, as the planet gears turn in opposite directions, the rotation of one of the two must be reversed to have the two produce the tilt motion.

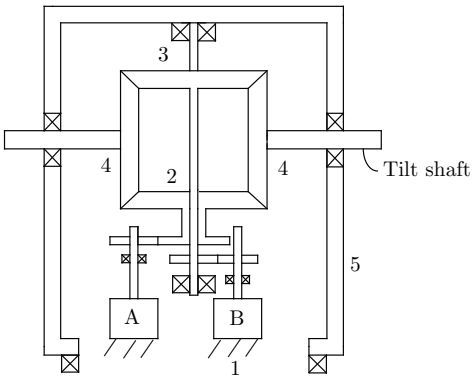

Figure 7: Differential gear train mechanism

6. **Hervé's pan-tilt linkage**

Hervé (2006) synthesized several two-limb parallel PTMGs using group theory. As the mechanisms proposed in (Hervé, 2006) are not overconstrained, manufacturing and assembly errors can be tolerated. Moreover, the pan and the tilt actuations are uncoupled, i.e., the pan and the tilt axes can be actuated independently. The first limb of the PTMGs proposed in (Hervé, 2006) comprises two revolutes with orthogonal axes in series, similar to a serial PTMG. The first revolute, which is active, of vertical axis, produces the pan motion, while the axis of the second revolute, which is passive, is horizontal, thereby producing the tilt. To obtain a PTMG, the second limb has to produce the whole six-dimensional displacement subgroup. Relations from group theory are used so as to achieve various two-limb parallel PTMGs, one of them being shown in Fig. 8; the actuated joints are shaded in the figure. It is noteworthy that the first three revolutes in the second limb produce the planar subgroup with normal parallel to the pan axis. The interested reader is referred to (Hervé, 2006) for more details.

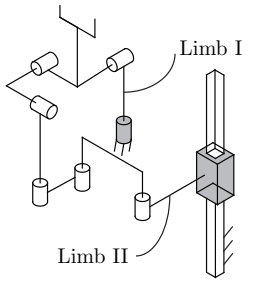

Figure 8: A two-limb parallel PTMG

3 Complexity Analysis

In any design task, like the problem at hand, a number of solutions are usually produced at the conceptual design stage from brainstorming sessions. The different alternatives resulting may all satisfy the functional requirements, but the designer has to compare them in order to select the most suitable one to go to the embodiment phase. Hence, an appropriate index, which gives a quantitative measure of the suitability of each alternative at the conceptual design stage, is required to serve as a basis for comparison.

Different algorithms of concept-evaluation have been studied in the literature. Khan (2007) developed a framework for the evaluation of mechanical systems based on the concept of *design complexity*, which closely relates to diversity of the design at hand. Robotic mechanical systems are composed of links, joints and actuators; to compute their complexity measures, the diversity of each of these components should be defined. For instance, the diversity of joint-types can be formulated by defining a parameter called the *loss of regularity* (LOR) of curves and surfaces (Khan et al., 2006). The LOR of a curve (surface) is the ratio of the 2-norm of the variations of its curvature—the root-mean-square (rms) value of the principal curvatures—to the 2-norm of the curvature—the rms value of the principal curvatures—itself. The LOR of a curve, p-LOR, is

$$\begin{aligned} \text{p-LOR} &\equiv \frac{\|\kappa'(\sigma)\|_2}{\|\kappa(\sigma)\|_2} \\ \|\kappa(\sigma)\|_2^2 = \int_0^1 \left[\kappa(\sigma)\right]^2 d\sigma,\ \|\kappa'(\sigma)\|_2^2 &= \int_0^1 \left[\kappa'(\sigma)\right]^2 d\sigma \end{aligned} \tag{10a}$$

where κ and $\sigma = s/l$ denote the curvature of the curve and the dimensionless coordinate along the curve, s and l being the path coordinate and the curve total length. The LOR of a surface, s-LOR, in turn, is

Table 1: The associated complexity measures of the various kinematic pairs

Joint type	R	P	H	SP	BV
Complexity (K_G)	0.0129	0.0249	0.0201	0.7392	1.0

$$\text{s-LOR} \equiv \left(\frac{Y}{\int_0^1 \int_0^1 \kappa_{\text{rms}}^2 d\sigma_1 d\sigma_2} \right)^{1/2}$$
$$Y \equiv \int_0^1 \int_0^1 \left[\left(\partial \kappa_{\text{rms}}/\partial \sigma_1\right)^2 + \left(\partial \kappa_{\text{rms}}/\partial \sigma_2\right)^2 \right] d\sigma_1 d\sigma_2 \tag{10b}$$

where κ_{rms}, σ_1 and σ_2 denote the rms value of the principal curvatures of the surface and two dimensionless path coordinates, respectively.

Kinematic pairs can be classified as lower and higher. The former connect two links along a common surface, the latter along a line or a point. In any event, contact between the two links takes place at points of two surfaces, each bounding one of the two links. Thus, to compute the complexity of the kinematic pairs, the s-LOR of their contact surfaces is recalled from (Khan, 2007; Khan et al., 2006). The complexity measures associated with the various kinematic pairs are obtained upon normalizing the LOR values, as tabulated in Table 1[1]. In this table, R, P and H denote the revolute, prismatic and helical pairs, SP and BV, in turn, denote the spur and bevel gears, respectively. The interested reader is referred to (Khan, 2007) for details.

The overall complexity of a robotic mechanical system is defined as a convex combination of its partial complexity measures, namely,

$$K = w_N K_N + w_L K_L + w_J K_J + w_B K_B + w_A K_A + w_H K_H \tag{11}$$

where w_X for $X = N, L, J, B, A, H$, are weights, which add up to unity, and K, K_N, K_L and K_J are overall, joint-number, loop and joint-type complexity measures; K_B, K_A and K_H are, in turn, link diversity, actuator-type complexity and actuator diversity, respectively. Each of these complexity measures is defined below:

1. Joint-Number Complexity K_N:

   The joint-number complexity K_N is defined as

   $$K_N = 1 - \exp(-q_N N) \tag{12}$$

   where N and q_N are, respectively, the total number of joints and a resolution parameter, to be described below.

2. Loop Complexity K_L:

   The loop complexity K_L is defined as

   $$K_L = 1 - \exp(-q_L L), \quad L = l - l_m \tag{13}$$

   where l, l_m and q_L are the number of loops, the minimum number of loops required to generate a given motion, and a resolution parameter, to be described below.

3. Joint-Type Complexity K_J:

   The joint-type complexity K_J is defined as

   $$K_J = \frac{1}{n} \left(n_R K_{G|R} + n_P K_{G|P} + n_H K_{G|H} + n_{SP} K_{G|SP} + n_{BV} K_{G|BV} \right) \tag{14}$$

[1]The LOR values giving rise to the complexity values of Table 1 are not identical to those of (Khan, 2007; Khan et al., 2006), but recalculated with some modifications; the details will be published in a forthcoming paper.

where n, n_R, n_P and n_H are the numbers of: lower and higher kinematic pairs; revolute, prismatic and helical joints; n_{SP} and n_{BV} are, in turn, the numbers of spur and bevel gear pairs, respectively, while $K_{G|X}$ is the geometric complexity associated with each kinematic pair.

4. Link Diversity K_B:

   The link diversity K_B is defined as

$$K_B = \frac{B}{B_{\max}}, \quad B = -\sum_{i=1}^{c} b_i \log_2 (b_i)$$
$$b_i = \frac{M_i}{\sum_{i=1}^{c} M_i} \tag{15}$$

   where M_i and c are, respectively, the number of occurrences of each type of geometric constraint between the links and their total number. The different geometric constraint types of binary links can be classified into five groups, based on the relative layout of the axes of their revolutes: 1) intersecting and perpendicular (M_1); 2) intersecting but not perpendicular (M_2); 3) parallel (M_3); 4) non-intersecting and perpendicular (M_4);
   5) non-intersecting but not perpendicular (M_5).

5. Actuator-Type Complexity K_A:

   The actuator-type complexity K_A is defined as

$$K_A = 1 - \exp(-q_A A), \quad A = a - a_m \tag{16}$$

   where a and a_m are the number of electromagnetic actuators and the minimum number required, respectively.

6. Actuator Diversity K_H:

   The actuator diversity K_H is defined as

$$K_H = \frac{H}{H_{\max}},\ H = -\sum_{i=1}^{d} \phi_i \log_2 (\phi_i),\ \phi_i = \frac{N_i}{\sum_{i=1}^{d} N_i} \tag{17}$$

   where N_i and d are, respectively, the number of occurrences of each actuator-type and their total number.

The resolution parameters used in the definition of the joint-number, the loop and the actuator-type complexity can be defined such that the maximum complexity attains a value of 0.9. Hence, the resolution parameters for $J = N, L, A$ are

$$q_J = \begin{cases} -\ln(0.1)/J_{max} & \text{for } J_{max} > 0 \\ 0 & \text{for } J_{max} = 0 \end{cases} \tag{18}$$

Now, to compute the complexity of the PTMGs described in Section 2, the required parameter of each alternative, such as the number of joints and loops, are listed in Table 2, where D_i, for $i = 1, \ldots, 6$, represents the six design variants introduced in Section 2, in the same order. The design with the Rzeppa joints is left out of the discussion because of its obvious complexity. Next, the resolution parameters are computed, as recorded in Table 3. Having assigned equal weights to the different complexity measures, the overall complexity of the design variants are computed and tabulated in Table 4. The top three designs are the five-bar linkage, the double universal joint and the bevel gear mechanisms.

Table 2: Design parameters required to compute the complexity measures

Variants	N	n_R	n_P	n_H	n_{SP}	n_{BV}	l
D1	7	4	0	0	2	1	2
D2	10	8	0	0	2	0	2
D3	9	6	0	1	2	0	2
D4	8	6	0	0	2	0	2
D5	10	6	0	0	2	2	2
D6	8	7	1	0	0	0	1

Variants	l_m	c	M_1	M_2	M_3	M_4	M_5
D1	0	2	0	2	3	0	0
D2	0	2	4	0	4	0	0
D3	0	2	1	0	6	0	0
D4	0	3	1	3	3	0	0
D5	0	2	0	3	4	0	0
D6	0	2	3	0	4	0	0

Variants	a	a_m	d	N_1	N_2		
D1	2	2	1	2	0		
D2	2	2	1	2	0		
D3	2	2	1	2	0		
D4	2	2	1	2	0		
D5	2	2	1	2	0		
D6	2	2	2	1	1		

Table 3: Resolution parameters

Variants	N	L	B	A	H
D1	7	2	0.9710	0	0
D2	10	2	1.0	0	0
D3	9	2	0.5917	0	0
D4	8	2	1.4488	0	0
D5	10	2	0.9852	0	0
D6	8	1	0.9852	0	1
q_J	0.2303	1.1513	-	0	-

Table 4: complexity measures of the different PTMGs

Variants	D1	D2	D3	D4	D5	D6
K_N	0.8005	0.9	0.8742	0.8416	0.9	0.8416
K_L	0.9	0.9	0.9	0.9	0.9	0.6835
K_J	0.3614	0.1581	0.1751	0.1944	0.3555	0.0144
K_B	0.4182	0.4307	0.2548	0.6240	0.4243	0.4243
K_A	0	0	0	0	0	0
K_H	0	0	0	0	0	1.0
K	0.4133	0.3981	0.3673	0.4266	0.4299	0.4939

4 Conclusions

In this report, several parallel PTMGs with their actuators mounted on the base platform were analyzed quantitatively using a complexity measure.

At the conceptual stage of any design problem, a few variants are usually obtained from brainstorming sessions. Then, a criterion is required to choose the most suitable alternative to go through the balance of the design process without relying on a parameteric model. To this end, the concept of design complexity

is recalled. The design complexity of a solution relates to the diversity of its components, namely, joints, links and actuators; the more diverse a solution, the more complex it is. Different complexity measures were defined based on the diversity of the various components. The overall complexity of a design alternative was computed as a convex combination of all of the partial complexity measures.

The parallel PTMG alternatives are ranked upon applying the concept of design complexity. The winning mechanism, whose complexity is a minimum, turns out to be a novel mechanism, introduced in this report, which includes a planetary gear train to produce the pan motion and a five-bar linkage of the RHRRR type to produce the tilt motion out of the rotation of the planet about the vertical axis. According to Hervé's classification, this five-bar linkage belongs to the class of exceptional mechanisms. Using group theory, it becomes apparent that the mechanism has a DOF of unity.

Bibliography

Angeles, J. (2004), 'The qualitative synthesis of parallel manipulators', *ASME Journal of Mechanical Design* **126**, 617–624.

Bellomo, N. and Montanari, P. (1978), 'The general theory of the mechanics of a large class of multi-bodied systems for constant velocity transmission between intersecting axes', *Mechanism and Machine Theory* **13**, 361–368.

Carricato, M. and Parenti-Castelli, V. (2004), 'A novel fully decoupled two-degree-of-freedom parallel wrist', *The international Journal of Robotics Research* **23**, 661–667.

Gogu, G. (2005), Fully-isotropic over-constrained parallel wrists with two degrees of freedom, *in* 'Proc. of the IEEE International Conference on Robotics and Automation', Barcelona, Spain.

Hervé, J. (1978), 'Analyse structurelle des mécanismes par groupes de déplacements', *Mechanism and Machine Theory* **13**, 437–450.

Hervé, J. (2006), 'Uncoupled actuation of pan-tilt wrists', *IEEE Transaction on Robotics* **22**(1), 56–64.

Hyman, B. (2003), *Fundamentals of Engineering Design*, Pearson Education, Sadddle River, N.J.

Iwashita, S. and Asada, T. (2005), Developing a service robot, *in* 'Proc. of the IEEE International Conference on Mechatronics and Automation', Niagara Falls, Ontario.

Johnson, D. A. and Willems, P. Y. (1993), 'On the necessary and sufficient conditions for homokinetic transmission in chains of cardan joints', *ASME Journal of Mechanical Design* **115**, 255–261.

Khan, W. A. (2007), *The Conceptual Design of Robotic Architectures Using Complexity Criteria*, PhD thesis, Department of Mechanical Engineering, McGill University, Montreal, Canada.

Khan, W. A., Caro, S., Pasini, D. and Angeles, J. (2006), Complexity analysis for the conceptual design of robotic architectures, *in* 'Proc. of 10th Advances in Robot Kinematics', Springer, Ljubljana, Slovenia, pp. 359–368.

Morozov, A. and Angeles, J. (2007), 'The mechanical design of a novel Schönflies-motion generator', *Robotics and Computer-Integrated Manufacturing* **23**, 82–93.

Pahl, G., Beitz, W. and Feldhusen, J. (2007), *Engineering Design: A Systematic Approach*, Springer, London-New York.

Pugh, S. (1991), *Total Design: Integrated Methods for Successful Product Engineering and Value Tradeoffs*, Wiley, New York.

Rzeppa, A. (1934), 'Universal joint', *United States Patent Office* .

Saaty, T. (1980), *The Analytic Hierachy Process*, McGraw-Hill Book Co., New York.

Vertechy, R. and Parenti-Castelli, V. (2006), 'Synthesis of 2-dof spherical fully parallel mechanisms', *Advances in Robot Kinematics* pp. 385–394.